DOI: 10.7589/JWD-D-23-00083

Journal of Wildlife Diseases, 60(2), 2024, pp. 298–305

Validation of a Field-Portable, Handheld Real-Time PCR System for Detecting *Pseudogymnoascus destructans*, the Causative Agent of White-Nose Syndrome in Bats

Sabrina S. Greening,[1,8] Katie Haman,[1,2] Tracy Drazenovich,[3] Maria Chacon-Heszele,[4] Michael Scafini,[5] Greg Turner,[5] John Huckabee,[6] Jean Leonhardt,[6] Jesse vanWestrienen,[4] Max Perelman,[4] Patricia Thompson,[2] and M. Kevin Keel[7]

[1] Department of Pathobiology, Wildlife Futures Program, University of Pennsylvania School of Veterinary Medicine, New Bolton Center, 382 West Street Road, Kennett Square, Pennsylvania 19348, USA
[2] Washington Department of Fish and Wildlife, 1111 Washington Street, Olympia, Washington 98501, USA
[3] One Health Institute, School of Veterinary Medicine, University of California, 1089 Veterinary Medicine Drive, Davis, California 95616, USA
[4] Biomeme, 401 North Broad Street, Suite 222, Philadelphia, Pennsylvania 19108, USA
[5] Bureau of Wildlife Management, Pennsylvania Game Commission, 2001 Elmerton Avenue, Harrisburg, Pennsylvania 17110, USA
[6] PAWS Wildlife Center, 15305 44th Avenue West, Lynnwood, Washington 98087, USA
[7] Department of Veterinary Medicine, Pathology, Microbiology, Immunology, School of Veterinary Medicine, University of California, 1089 Veterinary Medicine Drive, Davis, California 95616, USA
[8] Corresponding author (email: sgreenin@vet.upenn.edu)

ABSTRACT: White-nose syndrome (WNS), caused by the fungus *Pseudogymnoascus destructans*, has decimated bat populations across North America. Despite ongoing management programs, WNS continues to expand into new populations, including in US states previously thought to be free from the pathogen and disease. This expansion highlights a growing need for surveillance tools that can be used to enhance existing monitoring programs and support the early detection of *P. destructans* in new areas. We evaluated the feasibility of using a handheld, field-portable, real-time (quantitative) PCR (qPCR) thermocycler known as the Biomeme two3 and the associated field-based nucleic acid extraction kit and assay reagents for the detection of *P. destructans* in little brown bats (*Myotis lucifugus*). Results from the field-based protocol using the Biomeme platform were compared with those from a commonly used laboratory-based qPCR protocol. When using dilutions of known conidia concentrations, the lowest detectable concentration with the laboratory-based approach was 108.8 conidia/mL, compared with 1,087.5 conidia/mL (10 times higher, i.e., one fewer 10× dilution) using the field-based approach. Further comparisons using field samples suggest a high level of concordance between the two protocols, with positive and negative agreements of 98.2% and 100% respectively. The cycle threshold values were marginally higher for most samples using the field-based protocol. These results are an important step in establishing and validating a rapid, field-assessable detection platform for *P. destructans*, which is urgently needed to improve the surveillance and monitoring capacity for WNS and support on-the-ground management and response efforts.

Key words: Biomeme, field surveillance, *Pseudogymnoascus destructans*, white-nose syndrome.

INTRODUCTION

Since the emergence of white-nose syndrome (WNS) in 2006 (Blehert et al. 2009), many bat populations in North America have experienced rapid population declines, and several once-common species are now threatened with regional extinction (Frick et al. 2010; Ingersoll et al. 2013; Cheng et al. 2021). The cause of WNS is *Pseudogymnoascus destructans* (formerly *Geomyces destructans*; Gargas et al. 2009), a psychrophilic fungus adapted to infecting the epidermal tissue of bats, most noticeably on muzzles, ears, and wings (Warnecke et al. 2012). In response to the devastating effects of WNS, large investments have been and continue to be made toward a number of surveillance and monitoring programs, research projects, and management activities (Bernard et al. 2020). Nevertheless, *P. destructans* continues to spread. In 2022, it was detected in 43 US states and eight Canadian provinces (US Fish and Wildlife Service 2023), with the most recent detections in New Mexico (Bureau of Land Management 2021), Louisiana (Louisiana Department of Wildlife and Fisheries 2022), Idaho (Idaho

Fish and Game 2022), and Colorado (Colorado Parks and Wildlife 2022). In some species and in some hibernacula, mortality rates associated with WNS have been as high as 95–100% (Hoyt et al. 2021).

Across the eastern half of North America, surveillance for *P. destructans* and WNS has focused primarily on screening hibernating bats, with a high reliance on visual surveys and the collection of potentially infected bats for histopathologic examination (Janicki et al. 2015). These methods are not without limitations; the fungus may not always be visible on infected bats, potentially resulting in misdiagnosis and in missed opportunities to manage pathogen and disease spread (Meteyer et al. 2009). More recently, the development of real-time (quantitative) PCR (qPCR) for *P. destructans* has enabled the use of epidermal swabs to help detect the presence of the pathogen with greater sensitivity (Muller et al. 2013; Shuey et al. 2014). However, these assays still rely on laboratory testing that increases costs and delays the time to detection by a week or more, further delaying management actions.

In addition to the lack of tools that support the rapid detection of *P. destructans* in the field, many of the current surveillance programs are limited in the ability to detect the disease in bat populations that do not aggregate in observable roosts during hibernation or where the location of roosts remains unknown. For example, in many regions in the American Pacific Northwest, there is a distinct lack of large aggregations of hibernating bats, thus making it difficult to conduct ongoing surveillance. Consequently, much of what is known in regard to the transmission of *P. destructans* comes from data collected from bat populations located in the northeastern US (Lorch et al. 2010; Flory et al. 2012; Maher et al. 2012) and does not account for regional differences among bat hibernacula that may be key in understanding the potential impacts of the disease (Meierhofer et al. 2021). The difficulty in finding hibernacula remains a challenge; however, with the use of field-based tools, there is increased potential to sample opportunistically instead of relying solely on surveys of known roosts. In the state of Washington, US, the first case of WNS was confirmed in King County in 2016; however, the fungus continues to spread, with new cases confirmed in Benton County and Jefferson County for the first time in 2023 (Washington Department of Fish and Wildlife 2023). The continued spread of WNS in Washington highlights the need for a modified approach to allow for early, rapid detection of *P. destructans* both in new areas and across different habitats.

We aimed to evaluate the feasibility of using the two3 mobile thermocycler (Biomeme, Philadelphia, Pennsylvania, USA) for the rapid detection of *P. destructans* in a field setting. This handheld, battery-operated qPCR device can deliver PCR results on a smartphone. To evaluate the field-based approach, we compared the results from the Biomeme platform with those from a benchtop molecular approach commonly used by diagnostic laboratories conducting *P. destructans* surveillance.

MATERIALS AND METHODS

Validation and sensitivity testing

Before field sampling, banked samples known to be positive for *P. destructans* were used to validate the field-based extraction and qPCR protocol in a laboratory setting. We used 20 samples to compare the M1 Sample Prep Kit for DNA extraction (Biomeme) with the DNeasy Blood & Tissue Kit (Qiagen, Valencia, California, USA), while 10 samples were used to compare the Biomeme 10× DNA master mix (representing a 10× resuspended solution of the LyoDNA 2.0 Master Mix, Biomeme) and the Qiagen DNA master mixes (QuantiFast™ Probe PCR+ROX Vial Kit, Qiagen) with all assays run on the Applied Biosystems (ABI) 7500 Fast Real-Time PCR System (Waltham, Massachusetts, USA) at the University of California, School of Veterinary Medicine Diagnostic Laboratory (Davis, California, USA). To further evaluate the sensitivity of the field-based protocol (using the Biomeme extraction kit, the Biomeme master mix, and the Biomeme two3™ thermocycler PCR system) compared with the benchtop protocol (using the Qiagen extraction kit and master mix and the ABI PCR

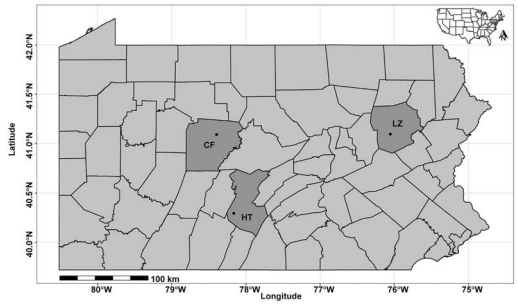

FIGURE 1. Map showing the trapping locations for little brown bats (*Myotis lucifugus*) within the counties of Luzerne (LZ), Clearfield (CF), and Huntingdon (HT), Pennsylvania, USA.

system), we compared cycle threshold (Ct) values following qPCR amplification of serially diluted test samples with a known concentration of *P. destructans* conidia. For the serial dilutions, conidia were enumerated using a hemocytometer, followed by a 12-step 1:10 dilution series, with all dilutions run in duplicate.

Sample collection for field comparison

After validation in the laboratory, we performed a direct comparison between the field-based protocol and the benchtop protocol in the field. This project underwent review by the Wildlife Health Section at the Washington Department of Fish and Wildlife to ensure animal welfare standards were upheld when handling live animals. To collect samples, 1.8-m-wide harp traps (Faunatech Austbat, Rydalmere, New South Wales, Australia) were used across three sites located in the counties of Luzerne, Clearfield, and Huntingdon, Pennsylvania, US (Fig. 1) to catch little brown bats (*Myotis lucifugus*). These sites were selected as they were known to be positive for *P. destructans* based on annual surveys. The presence of *P. destructans* was further confirmed at each site before the study with a single specimen sent to the US Geological Survey National Wildlife Health Center (Madison, Wisconsin, USA) for testing following their recommended guidelines. At each site, trapping occurred over 10 separate evenings between 26 April 2017 and 6 July 2017. The sites were near bat boxes, where little brown bats were known to roost and *P. destructans* or WNS had previously been detected. Two traps were used at each site. They were placed approximately 1 h before official sunset on each side of the bat boxes that were thought to contain the largest number of animals, based on a visual inspection. The traps were left standing until 30 min after sunset, at which time the traps were removed from the vicinity of the bat boxes. Following trapping, bats were bagged individually to await processing with the exception that all juveniles and pregnant females were released.

For each bat, two sampling protocols were used, one to collect swabs for the field-based protocol and another to collect swabs for the benchtop protocol. For the field-based protocol, three 1.2-cm-tip polyester swabs (Alpha TX743B, Texwipe, Moorpark, California, USA) were taken, including one from the right side of the muzzle, one across the dorsal surface of each extended wing, moving the swab from the body toward the outer margin of the patagium, and one along the back, moving the swab from head to tail. For each area, five swipes were taken (Fig. 2), ensuring that the swab was rotated a quarter turn with each stroke. All three swabs were then placed into a single tube containing a lysis buffer and shaken for 30 s. All swabs were stored in freezer boxes until all bats were sampled and further processing (i.e., extraction and qPCR) was completed in the field.

For the benchtop protocol, only a single swab (Alpha TX743B, Texwipe) was used, but multiple sites were swabbed, including the left side of the muzzle and across the dorsal surface of each extended wing, using the same approach as that for the field-based protocol (i.e., five strokes with a quarter turn). The number of swabs differed between the two protocols because the field-based extraction method required

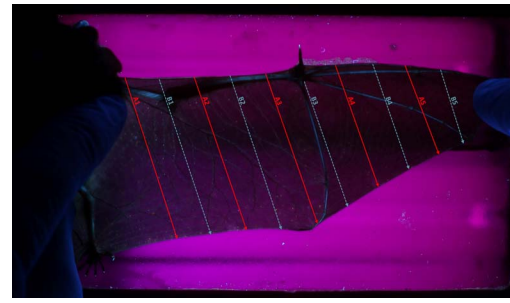

FIGURE 2. Placement of swab collection along the wing of little brown bats (*Myotis lucifugus*). For each field-based system swab, five swipes were taken, following lines A1 to A5 (red) for odd-numbered samples and lines B1 to B5 (blue) for even-numbered samples. In comparison, for the laboratory swabs, five swipes were taken, following lines A1 to A5 (red) for even-numbered samples and lines B1 to B5 (blue) for odd-numbered samples.

larger volumes of solutions; therefore, additional swabs were used to counteract potential dilution of the sample. As both sampling protocols required the muzzle and wings to be swabbed, an approach was used that alternated the site at which the swabs were taken from the wing (Fig. 2), while slightly different areas of the muzzles were swabbed for each protocol (left versus right). Standardizing the protocols in this way avoided having to sample multiple times over the same area on a single animal, minimizing differences in the sample quality between consecutive swabs. The single swab for the benchtop approach was stored in freezer boxes and placed on ice for delivery to the diagnostic laboratory (University of California, Davis). At each site, swabs were taken by the same field investigator over the 10 nights. Morphometric measurements (body weight and the length of the ear, tragus, forearm, and hindfoot) were recorded for each bat. All bats were banded to determine if recaptures occurred during future visits. After release, care was taken to ensure a new pair of gloves was used before handling the next bat.

Field-based extraction and qPCR protocol

All field-based samples were processed using a modified version of the manufacturer-recommended extraction and PCR protocol for the Biomeme M1 Sample Prep Kit for DNA. A copy of the final protocol has been provided (see Supplementary Material). To summarize, all three swabs taken from a bat were placed into a single tube containing 500 µL of Biomeme lysis buffer and shaken for 30 s. The DNA was extracted by drawing out the lysis buffer through the Biomeme sample prep column. This process was repeated 15 times. Next, two wash buffers (500 µL of Biomeme protein wash, followed by 750 µL of Biomeme wash buffer, were drawn through the column to help remove any impurities. This step was followed by an air-drying process in which air was rapidly pumped into the sample prep column for at least 20 pumps or until any remaining liquid had disappeared. Once dry, 1 mL of Biomeme elution buffer was drawn through the column for five pumps to release the DNA.

Following extraction, the assays were conducted using the Biomeme two3 thermocycler PCR system. Altogether, assays consisted of 17 µL of DNA extract, 2 µL of Biomeme proprietary 10× DNA master mix (representing a 10× resuspended solution of Biomeme's LyoDNA 2.0 Master Mix), and 1 µL of 20× primer and probe mix (primer at 0.8 µM and probe at 0.4 µM) that used the standard published primer sets for *P. destructans* PCR (Lorch et al. 2010). Initial denaturation occurred at 95 C for 3 min, followed by 40 cycles of denaturation at 95 C for 3 s, and annealing at 60 C for 30 s. Results were ready in approximately 45 min, with any reaction that crossed the threshold baseline within 40 cycles considered a positive. Negative controls were run during the first of each setup in the field but with only six wells and all samples being run in duplicate (i.e., three samples per run); it was decided that negatives would not be included in every run.

Benchtop extraction and qPCR protocol

All DNA extractions and qPCR protocols performed in the laboratory were completed as described (Muller et al. 2013). In brief, DNA extraction was initiated with a commercial kit (Gentra Puregene Genomic DNA Purification Kit, Qiagen) according to the manufacturer's instructions. Genomic DNA from the resulting lysate was further purified with a second kit (OmniPrep for Fungi, G-Biosciences, Maryland Heights, Missouri, USA), following the manufacturer's instructions beginning at the chloroform extraction step. Assays were conducted using the ABI 7500 Fast Real-Time PCR System with assays consisting of 5 µL of DNA extract, 12.5 µL of 2× Qiagen DNA master mix, 0.5 µL of 50× ROX dye solution, 0.5 µL of 20× forward and reverse primers (20 µM), and 0.25 µL of probe (primers and probe at 20 µM; QuantiFast Probe PCR+ROX Vial Kit, Qiagen). The PCR cycling conditions included an initial *Taq* polymerase activation step of 95 C for 3 min, followed by 40 cycles of denaturation at 95 C for 3 s and annealing at 60 C for 30 s. Similar to the field-based approach described earlier, any reactions that crossed the threshold baseline within 40 cycles were considered positive. Unlike the field-based approach, negative controls were run for all the benchtop assays.

Statistical analyses

Raw data were exported into R statistical software (version 4.0.5; R Core Team 2021) to estimate simple summaries, including the positive percent agreement and negative percent agreement of the field-based protocol when compared with the benchtop protocol. The Ct values for each assay were also plotted using the R package *ggstatsplot* (Patil 2021) to help

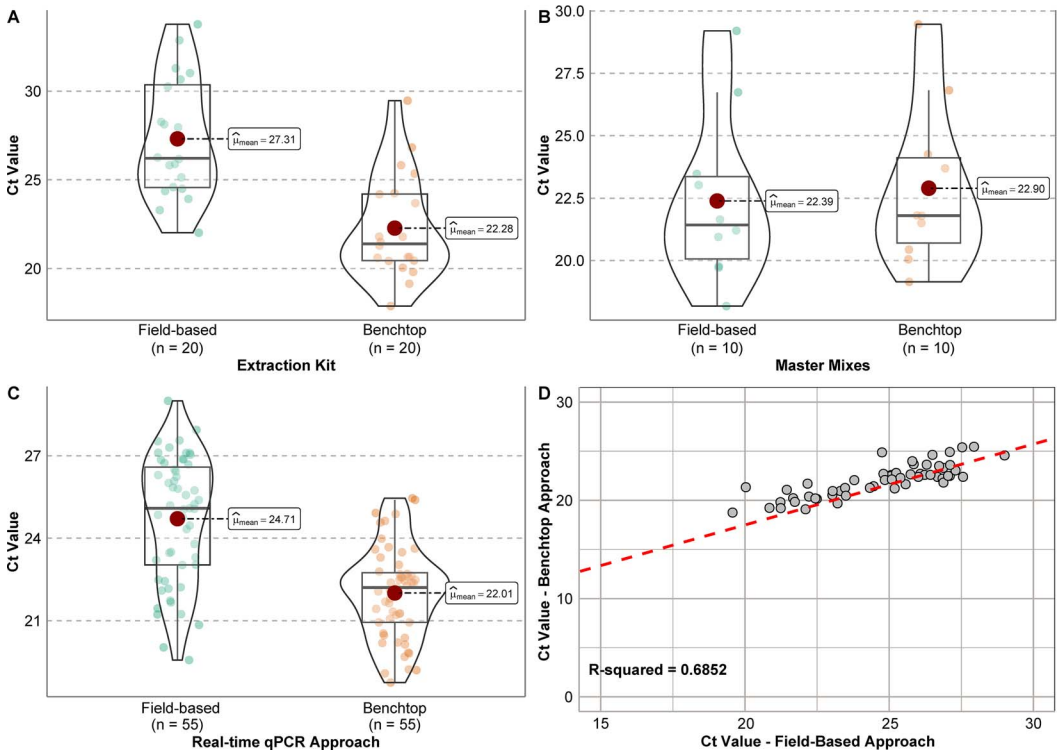

FIGURE 3. A comparison of the cycle threshold (Ct) values between assays using (A) different extraction kits, (B) different master mixes, and (C) real-time quantitative approaches. For the field-based approach, the M1 Sample Prep extraction kit (Biomeme), the 10× DNA master mix (Biomeme), and the two3 thermocycler PCR platform (Biomeme) were used. For the benchtop approach, the Qiagen DNeasy Blood & Tissue extraction kit, the QuantiFast Probe PCR+ROX Vial kit, and the Applied Biosystems 7500 Fast Real-Time PCR System were used. The agreement between sample Ct values for the field-based approach and the benchtop approach is shown in Plot D.

visualize the variance between the values for each sample. The plot was used to calculate the R^2 value based on a linear regression model. Paired *t*-tests were also performed to help determine if there was a significant difference between the sample Ct values using the field-based approach and the benchtop approach. Finally, the Cohen kappa statistic was calculated to estimate the level of agreement between the two detection methods and to test the null hypothesis that agreement was random (i.e., kappa statistic equals zero; Landis and Koch 1977).

RESULTS

During validation testing running all samples on the benchtop qPCR machine, for each set of paired samples, the protocols using the Biomeme extraction kit had higher Ct values than those using the Qiagen extractions kit (Fig. 3A), with a mean Ct value of 5.03 higher (minimum, 1.31 and maximum, 11.48; SD, 2.61; $P<0.0001$). Protocols using the Biomeme master mix had slightly lower Ct values between paired samples than those using the Qiagen master mix (Fig. 3B), with a mean difference of −0.51 (minimum, −0.08 and maximum, −0.97; SD, 0.32; $P=0.0007$). When using dilutions of known conidia concentrations, the lowest detectable concentration using the benchtop approach was 108.8 conidia/mL compared with 1,087.5 conidia/mL for the field system (Table 1).

For field testing, 137 little brown bats (not including juveniles or pregnant females) were captured, of which 87.6% (120/137; 63 males and 57 females) were sampled successfully according to the protocol. All morphometric measurements fell within the reference ranges

TABLE 1. Cycle threshold (Ct) values determined following real-time (quantitative) PCR amplification of serially diluted test samples with a known concentration of *Pseudogymnoascus destructans* conidia.

	Ct value[a]	
Conidia/mL	Benchtop protocol	Field-based protocol
5.44×10^5	26.43	26.08
2.72×10^5	28.4	26.51
1.36×10^5	29.15	28.49
1.09×10^5	30.72	29.65
1.09×10^4	32.82	33
1,087.5	34.92	33.47
108.75	37.68	0
10.88	0	0
1.09	0	0
0.11	0	0
0.011	0	0
0.0011	0	0

[a] Assays following the benchtop protocol in the laboratory used the Qiagen DNeasy Blood & Tissue extraction kit, the QuantiFast Probe PCR+ROX Vial kit, and the Applied Biosystems 7500 Fast Real-Time PCR System, while assays following the field-based protocol used the M1 Sample Prep extraction kit, the Biomeme10× DNA master mix, and the Biomeme two3 thermocycler PCR platform.

for little brown bats (see Supplementary Material Table S1). We found 46.7% (56/120) of the samples were positive using the benchtop protocol in comparison with 45.8% (55/120) using the field-based protocol. For the majority of positive samples (53/55, 96%), the field-based protocol had slightly higher Ct values between paired samples (Fig. 3C) with a mean difference of 2.70 (minimum, −0.13 and maximum, 5.17; SD, 1.29; $P<0.0001$). Overall, the positive percent agreement between the two approaches was 98.2% (95% confidence interval [CI], 90.6–99.7%), while the negative percent agreement was 100.0% (95% CI, 95.5–100.0%). This suggests a high level of concordance between the two protocols; this was also reflected in the Cohen kappa estimate of 0.985 (95% CI, 0.955–1.000).

DISCUSSION

Our study demonstrates that field results from the Biomeme two3 qPCR platform have a high level of concordance with real-time TaqMan PCR methods commonly performed in a laboratory setting to confirm the presence of *P. destructans* (Muller et al. 2013). Overall, Ct values were slightly higher using the field-base protocol, reflecting a decrease in sensitivity. This decrease in sensitivity might be a result of impurities in the extracted product, and due to the nature of field work, the risk of impurities may be higher. Alternatively, the decrease in sensitivity might be due to differences in the starting nucleic acid concentrations after extraction. A similar decrease in the sensitivity was seen when validating the protocols in a laboratory setting both when comparing the extraction kits (Fig. 3A) and the full protocols (Fig. 3C). Nevertheless, the field-based approach was still able to reliably detect *P. destructans* conidia at concentrations of 1,087.5 conidia/mL, a single 10-fold dilution less than the 108.8 conidia/mL using the benchtop approach. The reason for this 10-fold dilution difference remains unclear but note that a lower sensitivity would lead to a higher likelihood of false negatives. Therefore, if the field-based approach were to be used to test for the presence of the pathogen, it would be recommended to confirm the results using a diagnostic laboratory, particularly given the potential consequences of the disease if left undetected.

Since the completion of this study, Biomeme has upgraded their two3 system to the Franklin three9 thermocycler system. However, when designing the Franklin three9, Biomeme ensured that the new system was backward compatible with the same reagents used in this study. The main differences between the systems include the addition of a third color detection channel and an increase in the number of reaction wells, the maximum number of samples, and the maximum number of molecular targets per test run. A side-by-side comparison of the specifications for the two3 and Franklin three9 is provided (see Supplementary Material Table S2). The similarity in technology and reagents between the two systems make it unlikely that the results shown in this study would differ significantly if repeated using the new model; however, further work is needed to confirm the comparability between the two systems.

The establishment and validation of a rapid, field-assessable detection assay for *P. destructans* has the potential to significantly improve on-the-ground management and response efforts, as the time from sampling to results is drastically reduced. Such assays would have great value as a screening tool in regions where *P. destructans* has yet to be detected; due to portability, they could be used opportunistically or as tools to support visual surveys. This could enhance field efforts, improve biosecurity practices, and lead to more directed surveillance and monitoring for *P. destructans* and WNS. For example, many agencies have gear dedicated to sites known to be positive for *P. destructans* versus those sites thought to be negative. Knowing if a site has switched status in real time would help those in the field know when it is appropriate to switch gear and implement heightened disinfection and biosecurity procedures associated with positive sites, in addition to guiding further sampling for confirmatory diagnostic testing. Nevertheless, considering the slight differences in the detection levels between the field-based and laboratory-based assay and the fact that the Biomeme platforms are not considered diagnostic tools, it is recommended that any field results, positive or negative, be confirmed by a diagnostic laboratory.

The accessibility of the Biomeme platforms also provides an opportunity to extend the surveillance and monitoring for *P. destructans* to settings that would help screen for the pathogen outside of hibernating bats, such as in wildlife rehabilitation facilities that commonly encounter bat species, especially during winter months when the bats may be more likely to be positive for *P. destructans*. Such a field-based detection tool could help guide animal care decisions and biosecurity practices in wildlife rehabilitation facilities. For example, many bats end up in rehabilitation facilities due to significant wing damage. In these cases, while waiting for test results for *P. destructans,* which may take several weeks, the rehabilitator is implementing strict quarantine and biosecurity measures with huge implications for staff and resources. If animals tested negative for *P. destructans* on intake, these resources could be spared. Conversely, in instances where bats test positive for *P. destructans* on intake, rehabilitators would be able to apply strict biosecurity measures or make a more data-driven decision for euthanasia. Rehabilitation facilities would have to weigh up the costs of buying the instrument and running the assay themselves; however, the rapid detection of *P. destructans* has huge clinical relevance to the health of these animals, so these costs might be justified, as it would help maintain the health of other bats in care. Wildlife rehabilitators are also in a unique position to participate in disease monitoring by caring for a random sampling of wild animals (Yabsley 2019). Getting data from these animals could improve the ability to assess the population status, pathogen trends, and potential risks of spread in a region, while providing information for data-driven management actions to conserve North American bats in the face of this devastating disease.

ACKNOWLEDGMENTS

We extend our gratitude to Abigail Tobin at the Washington Department of Fish & Wildlife for help coordinating the project and PAWS Wildlife Center staff for contributions to sample processing. S. Greening was supported by the Robert J. Kleberg, Jr. and Helen C. Kleberg Foundation.

SUPPLEMENTAL MATERIAL

Supplementary material for this article is online at http://dx.doi.org/10.7589/JWD-D-23-00083.

LITERATURE CITED

Bernard RF, Reichard JD, Coleman JTH, Blackwood JC, Verant ML, Segers JL, Lorch JM, White JP, Moore MS, et al. 2020. Identifying research needs to inform white-nose syndrome management decisions. *Conserv Sci Pract* 2:e220.

Blehert DS, Hicks AC, Behr M, Meteyer CU, Berlowski-Zier BM, Buckles EL, Coleman JTH, Darling SR, Gargas A, et al. 2009. Bat white-nose syndrome: An emerging fungal pathogen? *Science* 323:227.

Bureau of Land Management. 2021. *Fungus causing bat disease found in eastern New Mexico*. https://www.blm.gov/press-release/fungus-causing-bat-disease-found-eastern-new-mexico. Accessed September 2022.

Cheng TL, Reichard JD, Coleman JTH, Weller TJ, Thogmartin WE, Reichert BE, Bennett AB, Broders

HG, Campbell J, et al. 2021. The scope and severity of white-nose syndrome on hibernating bats in North America. *Conserv Biol* 35:1586–1597.

Colorado Parks and Wildlife. 2022. *Fungus linked to fatal bat disease found in southeastern Colorado*. https://cpw.state.co.us/aboutus/Pages/News-Release-Details.aspx?NewsID=3572. Accessed September 2022.

Flory AR, Kumar S, Stohlgren TJ, Cryan PM. 2012. Environmental conditions associated with bat white-nose syndrome mortality in the north-eastern United States. *J Appl Ecol* 49:680–689.

Frick WF, Pollock JF, Hicks AC, Langwig KE, Reynolds DS, Turner GG, Butchkoski CM, Kunz TH. 2010. An emerging disease causes regional population collapse of a common North American bat species. *Science* 329:679–682.

Gargas A, Trest MT, Christensen M, Volk TJ, Blehert DS. 2009. *Geomyces destructans* sp. nov. associated with bat white-nose syndrome. *Mycotaxon* 108:147–154.

Hoyt JR, Kilpatrick AM, Langwig KE. 2021. Ecology and impacts of white-nose syndrome on bats. *Nat Rev Microbiol* 19:196–210.

Idaho Fish and Game. 2022. *Fungus that causes white-nose syndrome detected in three Idaho bat species at Minnetonka Cave*. https://idfg.idaho.gov/press/fungus-causes-white-nose-syndrome-detected-three-idaho-bat-species-minnetonka-cave/. Accessed September 2022.

Ingersoll TE, Sewall BJ, Amelon SK. 2013. Improved analysis of long-term monitoring data demonstrates marked regional declines of bat populations in the eastern United States. *PLoS One* 8:e65907.

Janicki AF, Frick WF, Kilpatrick AM, Parise KL, Foster JT, McCracken GF. 2015. Efficacy of visual surveys for white-nose syndrome at bat hibernacula. *PLoS One* 10: e0133390.

Landis JR, Koch GG. 1977. The measurement of observer agreement for categorical data. *Biometrics* 33:159–174.

Lorch JM, Gargas A, Meteyer CU, Berlowski-Zier BM, Green DE, Shearn-Bochsler V, Thomas NJ, Blehert DS. 2010. Rapid polymerase chain reaction diagnosis of white-nose syndrome in bats. *J Vet Diagn Invest* 22:224–230.

Louisiana Department of Wildlife and Fisheries. 2022. *LDWF: Fungus that causes white-nose syndrome in bats detected in Louisiana*. https://www.wlf.louisiana.gov/news/ldwf-fungus-that-causes-whitenose-syndrome-in-bats-detected-in-louisiana. Accessed September 2022.

Maher SP, Kramer AM, Pulliam JT, Zokan MA, Bowden SE, Barton HD, Magori K, Drake JM. 2012. Spread of white-nose syndrome on a network regulated by geography and climate. *Nat Commun* 3:1306.

Meierhofer MB, Lilley TM, Ruokolainen L, Johnson JS, Parratt SR, Morrison ML, Pierce BL, Evans JW, Anttila J. 2021. Ten-year projection of white-nose syndrome disease dynamics at the southern leading-edge of infection in North America. *Proc R Soc B* 288:e20210719.

Meteyer CU, Buckles EL, Blehert DS, Hicks AC, Green DE, Shearn-Bochsler V, Thomas NJ, Gargas A, Behr MJ. 2009. Histopathologic criteria to confirm white-nose syndrome in bats. *J Vet Diagn Invest* 21:411–414.

Muller LK, Lorch JM, Lindner DL, O'Connor M, Gargas A, Blehert DS. 2013. Bat white-nose syndrome: A real-time TaqMan polymerase chain reaction test targeting the intergenic spacer region of *Geomyces destructans*. *Mycologia* 105:253–259.

Patil I. 2021. Visualizations with statistical details: The "ggstatsplot" approach. *J Open Source Softw* 6:3167–3172.

R Core Team. 2021. *R: A language and environment for statistical computing*. R Foundation for Statistical Computing, Vienna, Austria. https://www.R-project.org/. Accessed March 2022.

Shuey MM, Drees KP, Lindner DL, Keim P, Foster JT. 2014. Highly sensitive quantitative PCR for the detection and differentiation of *Pseudogymnoascus destructans* and other *Pseudogymnoascus* species. *Appl Environ Microbiol* 80:1726–1731.

US Fish and Wildlife Service, White-Nose Syndrome Response Team. 2023. *Where is WNS now*? https://www.whitenosesyndrome.org/where-is-wns. Accessed September 2022.

Warnecke L, Turner JM, Bollinger TK, Lorch JM, Misra V, Cryan PM, Wibbelt G, Blehert DS, Willis CKR. 2012. Inoculation of bats with European *Geomyces destructans* supports the novel pathogen hypothesis for the origin of white-nose syndrome. *Proc Natl Acad Sci U S A* 109:6999–7003.

Washington Department of Fish and Wildlife. 2023. *White-nose syndrome and bat-killing fungus detected in two new Washington counties*. https://wdfw.wa.gov/newsroom/news-release/white-nose-syndrome-and-bat-killing-fungus-detected-two-new-washington-counties. Accessed October 2023.

Yabsley MJ. 2019. The role of wildlife rehabilitation in wildlife disease research and surveillance. In: *Medical management of wildlife species: A guide for practitioners*, Hernandez SM, Barron HW, Miller EA, Aguilar RF, Yabsley MJ, editors. Wiley, Hoboken, New Jersey, pp. 159–165.

Submitted for publication 9 May 2023.
Accepted 2 January 2024.